Theoretical Investigation of Steric and Electronic Effects of *meso*-Phenyl on Co-Porphyrin Catalyzed Activation of Dioxygen

NIAN LIU, DENG WEI, GUO-FANG JIANG and CAN-CHENG GUO[*]

College of Chemistry and Chemical Engineering, Hunan University, Changsha 410082, P.R. China

*Corresponding author: Fax: +86 731 8821488; Tel: +86 731 8821314; E-mail: ccguo@hnu.edu.cn; lkl7907@163.com

The molecule oxygen (O_2) activated on cobalt tetraphenylporphyrin (CoTPP) to form the peroxide species $CoTPPO_2$, which is the key intermediate in the behavior of metalloporphyrin catalyzed hydrocarbon oxidation, was simulated by the quantum chemical calculations. The effect of the *meso*-phenyl ring on the formation of the peroxide species $CoTPPO_2$ was investigated for the first time. The molecular geometry studies indicated that the *meso*-phenyl ring rotated with the molecule oxygen coordinated with CoTPP. Further nature atomic charge and nature bond orbital analysis supported that the steric changing of the *meso*-phenyl has a positive effect on the electron transport between CoTPP and O_2 to from the peroxide intermediate.

Keywords: Cobalt porphyrin, Oxygen, Catalyst, Quantum chemical.

INTRODUCTION

As a model of cytochrome P-450 mono-oxygenase, metalloporphyrin catalyzed hydrocarbon oxidation under mild condition has been studied systematically by many groups in the last decades[1-7]. Previous studies[8-11] showed that the molecular oxygen can be activated on metalloporphyrin surface to form the peroxide species MP-O_2. With the further O-O bond broken, the reactive intermediate [MP=O]$^{+\cdot}$ can be available to oxidate the C-H bond of the different kinds of hydrocarbon. It was observed that the intermediate [PFe^{IV}=O]$^{+\cdot}$ can be formed in the cytochrome P-450 catalyzed reaction by the EPR and the crystal studies[1]. Some theoretical studies[12,13] also supported the existence of the manganese oxo intermediate Mn=O. Since the importance of the peroxide species MP-O_2, a few papers have been published to describe the coordination of the metal ion and the molecular oxygen based on iron porphyrin and manganese porphyrin[14-34]. For example, an end-on configuration complexe FeP-O_2 was calculated by the density functional theory(DFT)[28] and the manganese oxo species MnP-O_2 was also simulated by DFT calculations[22].

In contrast to the fruitful reports of the center mental ion and the oxygen ligand, there are few reports to clarify the structure information of the peripheral substitutes such as *meso*-phenyl groups. But a lot of evidences have supported that the peripheral substitutes have significant influences on the properties of the metal porphyrins[29-31]. The catalytic activities of porphyrins have been proved to be linear correlation with the electrical properties of different peripheral substitutes by our group[31-33]. For better understanding the relevant law of the peripheral substitutes on porphyrin, the *meso*-phenyl groups on CoTPP was investigated on the distribution of the geometry structures and the electrons before and after the peroxide species $CoTPPO_2$ formed by the quantum chemical method.

EXPERIMENTAL

Calculation for structure of CoTPP: The initial geometry of CoTPP was built based on the crystal structure data with D_{4h} point group symmetry assumed[35]. The total energy and the electronic energy of two kinds of spin multiplicities (S = 1/2, 3/2) were calculated by semi-empirical PM3 implemented in the soft package Hyperchem 7.0 (Hypercube Inc., USA) to confirm the ground state of CoTPP. The Polak-Ribiere conjugate gradient algorithm was applied during the calculation[36-38]. Further DFT optimizations for CoTPP were performed Lee. Yang and Parr correlation (B3LYP) with the 6-311G basis set employed[39-41]. The optimized structure of CoTPP was show in Fig. 1.

Calculation for structure of peroxide species $CoTPPO_2$: At present, a few papers is reported to disclose the structure of the peroxide species MP-O_2 without the peripheral substitutes on the porphyrin ring such as FeP-O_2 and MnP-O_2. The substitutes such as the *meso*-phenyl rings were freezed or neglected to decrease the calculation consuming. The end-on and the
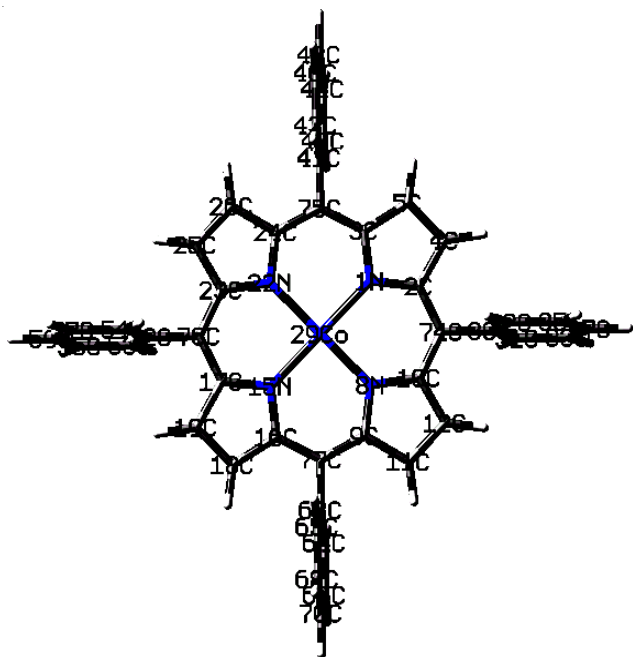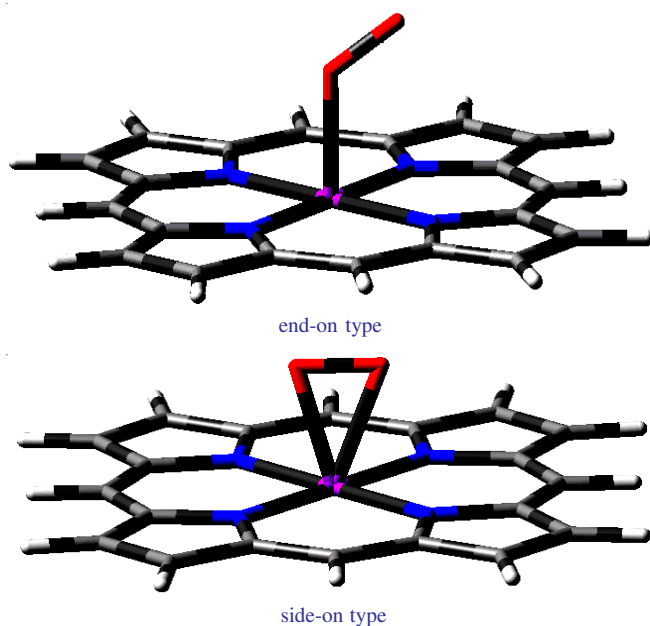
Fig. 1. Optimized structure of CoTPP

end-on type

side-on type

Fig. 2. Proposed intermediates for O_2 coordinate with metalloporphyrin

side-on configurations of the $PM-O_2$ shown in Fig. 2 can be available by these theoretical calculations[22,25,39].

In this paper, the original structure of the peroxide species $CoTPPO_2$ was built in both the end-on and the side-on configurations same as Fig. 2. The molecule oxygen was put above the center Co(II) ion at the distance about 3.0 Å with two different configurations. Cobalt(II) porphyrins commonly exist as the low spin electronic states differently and is insensitive to the ligand[40-47]. So $CoTPPO_2$ was considered as the low spin (S=1/2) statues. Further DFT geometry optimize calculations for $CoTPPO_2$ were performed at B3LYP/6-311G level without any geometry limits. The behavior of the *meso*-phenyl rings was also simulated. The natural atomic charges (NAC) and the natural bond orbital (NBO) parameters of CoTPP and $CoTPPO_2$ were also calculated accordingly. All of the DFT

studies were done on Dell 9150 PC (3.8GHz, 2GB) by using Gaussian03W soft package[44].

RESULTS AND DISCUSSION

The geometries of CoTPP in different spin multiplicities of S (1/2, 3/2) optimized by PM3 method are illustrated in Fig. 1. The energies listed in Table-1 indicate that the total energy of S = 1/2 state is about 52.75 kcal/mol lower than S = 3/2 state. So the ground electronic state of CoTPP is the low spin S = 1/2 which is same as the ESR experimental results reported by Liao *et al.*[40,45].

TABLE-1
ENERGIES IN DIFFERENT SPIN
MULTIPLICITIES OF CoTPP (kcal/mol)

Energy	S = 1/2	S = 3/2
Relative total energy	0.0000	52.75
Binding energy	-9534.89	-9482.14
Isolated atomic energy	-153775.73	-153775.73
Electronic energy	-1812372.20	-1830058.27
Core-core interaction	1649061.57	1666800.40

The DFT optimized structure parameters were partially summarized in Table-2. The structural data indicated that the DFT optimized structure of CoTPP is very close to the crystal structure. And the vibration frequency analysis has also been done on the optimized CoTPP and $CoTPPO_2$ to confirm the stability of these structures. A final end-on configuration of $CoTPPO_2$ is available after the DFT geometry optimization whatever the initial position of O_2 is the side-on or the end-on. It is different from those theory calculation results reported previously[22,25,39] which ignored the *meso*-phenyl rings during the analog computation.

As the optimized structures shown in Fig. 3, the macro cycle of CoTPP is almost a plane with the *meso*-phenyl rings perpendicular to it. With the axial O_2 ligand coordinated with
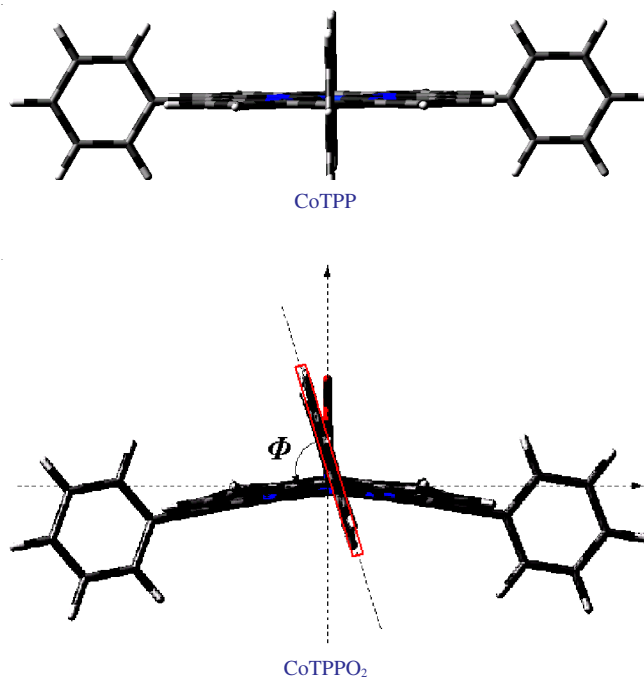

CoTPP

$CoTPPO_2$

Fig. 3. DFT optimized structures side view of CoTPdP and $CoTPPO_2$

TABLE-2 SOME OPTIMIZED STRUCTURE PARAMETERS OF CoTPP, CoTPPO$_2$ AND THE CRYSTAL DATA OF CoTPP				
Compound parameters of structure	CoTPP + O$_2$			CoTPPO$_2$ (end-on) B3LYP/6-311G
	PM3	B3LYP/6-311G	Crystal data [Ref. 23]	
Bond length (Å) N1-C2	1.425	1.395	1.387	1.393
N1-C3	1.426	1.395	1.378	1.394
C2-C4	1.438	1.444	1.426	1.444
C3-C5	1.438	1.444	1.384	1.445
C4-C5	1.373	1.359	1.346	1.360
Co29-N1	1.970	1.985	1.949	1.979
Co29-O79		3.0		2.053
O78-O79		1.256		1.312
Bond angle (°) ∠N1-Co29-N22	89.97	90.00	90.00	89.80
∠N1-Co29-N15	177.8	179.2	178.6	174.0
∠Co29-N1-C2	128.3	127.5	127.5	126.6
∠Co29-N1-C3	128.2	127.5	127.4	127.8
∠N1-C2-C4	110.8	110.3	110.4	109.9
∠Co29-O79-O78		135		122.2

the central Co atom, two obvious geometrical changes were happened on CoTPP. First, the macro cycle of CoTPP turned to be slight bending to form a saddle type which has been proved to be a low energy configuration. The second, the *meso*-phenyl rings rotated and formed a 74.5° dihedral angle (ϕ) with the macro cycle of CoTPP. At the same time, the axial O$_2$ ligand draw close to the central Co atom as the end-on configuration. The Co29-O79 distance decreased from 3.000 Å to 2.053 Å and the O78-O79 distance increased from 1.256 to 1.287 Å. The Co-O-O angle ∠Co29-O79-O78 of the final optimized CoTPPO$_2$ is about 122.2°. The geometrical data indicated that the O-O bond was weakened after the coordination, which means the O$_2$ was activated by CoTPP. The weakened O-O bond would be more easy to be broke and form the reactive intermediate TPPCo=O to oxidate the C-H bond of the hydrocarbons.

The optimized structures showed that the *meso*-phenyl rings of CoTPP were rotated when coordinated with the molecular O$_2$. There would be some steric effects for the active potential of cobalt porphyrin molecule. Further electrical analysis was performed to disclose the effects of these steric changes on CoTPP catalyzed activation of O$_2$. The nature atomic charges of the oxygen atoms were calculated while the dihedral angle (ϕ) was changed from 90° to 74.5°. It was obviously that the charges on the oxygen atoms were increased by -0.3792e with the rotation of the *meso*-phenyl rings. The π bond on the *meso*-phenyl ring would have some conjugative effect with the π-orbital on the macrocycle of CoTPP while the *meso*-phenyl ring rotated. There would be a part of electrons on the phenyl ring going through the porphyrin cycle and transferring to the centre Co atom while the Co atom combined with O$_2$ (Table-3).

The natural bond orbital (NBO) analysis results (Table-4) of CoTPP showed that the occupancies on $3d_{x^2-y^2}$ orbital of Co were increased from 0.5738e to 1.9765e after coordinated with the axial ligand O$_2$. Meanwhile, the occupancies on $3d_{xy}$ and $3d_{z^2}$ were decreased in some degree. The stabilizing energies of NBO analysis of CoTPPO$_2$ are listed in Table-5. It showed that the electron transfer from N atomic on porphyrin cycle to the central Co atom would be beneficial to the stability of the

TABLE-3 CALCULATED CHARGES OF CoTPPO$_2$ WITH ϕ ANGLE ROTATED PER 2°			
$\phi/(°)$	$q_{O(78)}$/(e)	$q_{O(79)}$/(e)	Δq/(e)
74.5°	-0.1574	-0.2218	-0.3792
76.5°	-0.1561	-0.2181	-0.3742
78.5°	-0.1533	-0.2145	-0.3678
80.5°	-0.1497	-0.2088	-0.3585
82.5°	-0.1434	-0.2035	-0.3469
84.5°	-0.1377	-0.1988	-0.3365
86.5°	-0.1287	-0.1914	-0.3201
88.5°	-0.1201	-0.1810	-0.3011
90.0°	-0.1154	-0.1620	-0.2774

TABLE-4 NATURAL ATOMIC ORBITAL OCCUPANCIES ANALYSIS FOR 3d-ORBITALS OF Co IN CoTPP AND CoTPPO$_2$					
Structure	$3d_{xy}$	$3d_{xz}$	$3d_{yz}$	$3d_{x^2-y^2}$	$3d_{z^2}$
CoTPP	1.9715	1.9371	1.9371	0.5738	0.9941
CoTPPO$_2$	0.6456	1.9405	1.9464	1.9765	0.7987

TABLE-5 PART OF CALCULATED RESULTS OF CoTPPO$_2$ BY NBO ANALYSIS			
Structure	Donor NBO (i)	Acceptor NBO (j)	ΔE/(kJ/mol)
CoTPPO$_2$	LP(1) N1	LP*(5) Co29	13.48
	LP(1)N1	LP*(6) Co29	20.73
	LP(1)N8	LP*(5) Co29	13.48
	LP (1) N8	LP*(6) Co29	20.73
	LP(1)N15	LP*(5) Co29	13.79
	LP (1) N15	LP*(6) Co29	21.04
	LP (1) N22	LP*(5) Co29	13.79
	LP(1)N22	LP*(6) Co29	21.04
	LP(3)Co29	BD*(1) O78-O79	4.83

coordiantion system and the electrons on the 3d-orbitals of Co also have the trend to transfer to the anti-bonding orbital of O$_2$. These theory calculations proved that the electron transfer direction can be described as phenyl $\to$ CoP $\to$ O$_2$. The steric changes of the *meso*-phenyl ring would enhanced the electron transfer from the phenyl ring to CoP cycle which will further be good to the activation of O$_2$. The *meso*-phenyl rotation

would be a positive action to promote CoTPP coordinate with the axial ligand O_2.

For the end-on configuration of the optimized $CoTPPO_2$, the molecular orbital theory put forward that the orbitals between the reactants should fit with symmetry. It is well known that the HOMO of O_2 is the π^* type orbital. It has the right symmetry to reacts with the d_{xy} orbital of the Co. The electron transfer from the d_{z^2} of Co to the σ^* type orbital of O-O bond are also fit in the symmetry. These electron transfer directions are also well consistent with the NBO calculation results (Tables 4 and 5). Tracing back to the geometry changes of $CoTPPO_2$, the Co-O-O bended to form an angle about $122.2°$. This geometry is favorable to the maximum overlap between the d_{z^2} of Co and the σ^* type orbital of O_2, as well as more effective to the interaction between the d_{xy} of Co and the π^* type orbital of O_2. Furthermore, the electron transfer from the p_z of N to the $d_{x^2-y^2}$ of Co is also allowed.

Conclusion

In summary, the quantum chemistry have been applied to investigate the molecular oxygen (O_2) activated on cobalt tetraphenylporphyrin (CoTPP). The stable end-on configuration of the complex $CoTPPO_2$ was available by the optimization. The geometrical structure of $CoTPPO_2$ showed that the *meso*-phenyl ring rotated when CoTPP coordinated with O_2 ligand. Further electrical analysis disclosed that this steric rotation would promote the electron transfer from the *meso*-phenyl ring to the CoP macro cycle, which would be beneficial to enhance the potential of CoTPP to activate the dioxygen. The molecular graphic studies also manifested that the weakened O-O bond was the portent of the final breakage of the O-O bond to form the TPPCo=O intermediate which is the key reactive species for the hydrocarbon oxidation. We believe all of these investigations will be useful for the future design of the novel high performance cobalt porphyrin catalyst.

REFERENCES

1. J.T. Groves and T.E. Nemo, *J. Am. Chem. Soc.*, **105**, 6243 (1983).
2. B. Meunier, *Chem. Rev.*, **92**, 1411 (1992).
3. C.A. Hasemann, R.G. Kurumbail, S.S. Boddupalli, J.A. Peterson and J. Deisenhofer, *Structure*, **3**, 41 (1995).
4. M.A. Schiavon, Y. Iamamoto, O.R. Nascimento and M.D. Assis, *J. Mol. Catal. A*, **174**, 213 (2001).
5. C.C. Guo, H.P. Li and J.B. Xu, *J. Catal.*, **185**, 345 (1999).
6. W.W. Nam, H.J. Lee, S.Y. Oh, C. Kim and H.G. Jang, *J. Inorg. Biochem.*, **80**, 219 (2000).
7. R.R.L. Martins, M.G.P.M.S. Neves, A.J.D. Silvestre, M.M.Q. Simoes, A.M.S. Silva, A.C. Tomé, J.A.S. Cavaleiro, P. Tagliatesta and C. Crestini, *J. Mol. Catal. A*, **172**, 33 (2001).
8. D. Hamdane, H.M. Zhang and P. Hollenberg, *Photosynth. Res.*, **98**, 657 (2008).
9. K. Dürr, B.P. Macpherson, R. Warratz, F. Hampel, F. Tuczek, M. Helmreich, N. Jux, and I. Ivanovic-Burmazovic, *J. Am. Chem. Soc.*, **129**, 4217 (2007).
10. F. Hiroshi, *Coord. Chem. Rev.*, **226**, 51 (2002).
11. M. Momenteau and C.A. Reed, *Chem. Rev.*, **94**, 659 (1994).
12. I. Shlichting, J.B. Berendzen, K. Chu, A.M. Stock, S.A. Maves, D.E. Benson, R.M. Sweet, D. Ring, G.A. Petsko and S.G. Sligar, *Science*, **287**, 1615 (2000).
13. R. Davydov, T.M. Makris and V. Kofman, *J. Am. Chem. Soc.*, **123**, 1403 (2001).
14. P.H. Toy, M. Newcomb and P.F. Hollenberg, *J. Am. Chem. Soc.*, **120**, 7719 (1998).
15. M. Newcomb and P.H. Toy, *Acc. Chem. Res.*, **33**, 449 (2000).
16. I.G. Denisov, T.M. Makris, S.G. Sligar and I. Schlichting, *Chem. Rev.*, **105**, 2253 (2005).
17. B. Meunier, S.P. de Visser and S. Shaik, *Chem. Rev.*, **104**, 3947 (2004).
18. J. Haber, L. Matachowski, K. Pamin and J. Poltowicz, *J. Mol. Catal. A*, **198**, 215 (2003).
19. D, Lahaye and J.T. Groves, *J. Inorg. Biochem.*, **101**, 1786 (2007).
20. J.T. Groves, in ed: P.R.O. de Montellano, Cytochrome P450: Structure, Mechanism and Biochemistry, Models and Mechanisms of Cytochrome P-450 action, Kluwer Academic/Plenum, New York, edn 3, p. 1/1-1/44 (2005).
21. P. Rydberg, E. Sigfridsson and U. Ryde, *J. Biol. Inorg. Chem.*, **9**, 203 (2004).
22. D. Rutkowska-Zbik and M. Witko, *J. Mol. Catal. A*, **275**, 113 (2007).
23. R.D. Bach and O. Dmitrenko, *J. Am. Chem. Soc.*, **128**, 1474 (2006).
24. A.N. Groenhof, A.W. Ehlers and K. Lammertsma, *J. Am. Chem. Soc.*, **129**, 6204 (2007).
25. D. Rutkowska-Zbik and M. Witko, *J. Mol. Catal. A*, **258**, 376 (2006).
26. D. Rutkowska-Zbik, R. Tokarz-Sobieraj and M. Witko, *J. Chem. Theory Comput.*, **3**, 914 (2007).
27. A.R. Shaikh, R. Sahnoun, E. Broclawik, M. Koyama, H. Tsuboi, N. Hatakeyama, A. Endou, H. Takaba, M. Kubo and C.A. Del. Carpio, *J. Inorg. Biochem.*, **103**, 20 (2009).
28. D. Harris, G. Loew and L. Waskell, *J. A. Chem. Soc.*, **120**, 4308 (1998).
29. A. B. Ormond, H.S. Freem, *Dyes Pigments.*, **96**, 440 (2013).
30. A. Zabardasti and M. Mirzaeian, *Asian J. Chem.*, **19**, 4753 (2007)
31. N. Liu, G. F. Jiang, C. C. Guo, Z. Tan, *J. Mol. Catal. A*, **304**, 40 (2009)
32. C.C. Guo, *J. Catal.*, **178**, 182 (1998).
33. C.C. Guo, Q. Liu, X.T. Wang and H.Y. Hu, *J. Mol. Catal. A*, **282**, 55 (2005).
34. Q. Jiang, Y. Xiao, Z. Tan, Q.H. Li and C.C. Guo, *J. Mol. Catal. A*, **285**, 162 (2008).
35. E. D. Stevens, *J. Am. Chem. Soc.*, **103**, 5087 (1981).
36. Q.Z. Lü, R.Q. Yu and G.L. Shen, *J. Mol. Catal. A*, **198**, 9 (2003).
37. A.I. Kuleff, S. Lünnemann and L.S. Cederbaum, *J. Chem. Phys. A*, **399**, 245 (2012).
38. Q.L. Wei, N. Liu, S.S. Zhang and X.M. Li, *Asian J. Chem.*, **18**, 1796 (2006).
39. M.C. Curet-Arana, G.A. Emberger, L.J. Broadbelt and R.Q. Snurr, *J. Mol. Catal. A*, **285**, 120 (2008).
40. M.S. Liao, J.D. Watts and M.J. Huang, *J. Phys. Chem. A*, **109**, 11996 (2005).
41. J.J.P. Stewart, *J. Comput. Chem.*, **10**, 209 (1989).
42. A.D. Beck, *J. Chem. Phys.*, **98**, 5648 (1993).
43. C. Lee, W. Yang and R.G. Parr, *Phys. Rev. B*, **37**, 785 (1988).
44. M.J. Frisch, G.W. Trucks and H.B. Schlegel, Gaussian 03, Revision: B.05; Gaussian, Inc., (2003).
45. W.C. Lin, *Inorg. Chem.*, **15**, 1114 (1976).
46. R. Zwaans, J.H. van Lenthe and D.H.W. den Boer, *J. Mol. Struct.*, **339**, 153 (1995).
47. R. Zwaans, J.H. van Lenthe and D.H.W. den Boer, *J. Mol. Struct.*, **367**, 15 (1996).